JOURNAL OF MATERIALS SCIENCE 9 (1974) 65–73

Esr linewidths in neodymium-doped calcium tungstate

G. BROWN, C. J. KIRKBY,* J. S. THORP
Department of Applied Physics and Electronics, University of Durham, UK

Electron spin resonance linewidths of Nd^{3+} in $CaWO_4$ at 35 GHz and 4.2 K are examined experimentally and theoretically for a range of Nd concentration. The derivative peak-to-peak linewidths, as determined experimentally, increase from 1.1 mT at 0.034% Nd to 4.1 mT at 0.816% Nd in vacancy-compensated single crystals at a polar angle of 90°. The homogeneous broadening is found to be owing almost exclusively to the Nd-Nd dipolar interaction, while the predominant inhomogeneous mechanism is due to a crystalline axis misorientation of 57 min of arc. Both the spin-lattice relaxation time and the linewidth show an anomaly at a polar angle of about 30°, indicating the presence of cross-relaxation to an impurity, probably cerium.

1. Introduction

Over the past fifteen years, the rare-earth doped Scheelites have received extensive study because, apart from affording the advantages of room-temperature laser operation in the particular case of Nd^{3+}:$CaWO_4$, an homologous series exists providing considerable opportunity for the systematic study of crystal field effects. Although there is a large volume of published data from electron spin resonance on rare-earth doped calcium tungstate, there appears to have been no investigation of the influence of the concentration of the paramagnetic ion on the resonance linewidths or spin-lattice relaxation times. This paper presents experimental results and calculations pertaining to homogeneous line-broadening mechanisms; by comparing these, the principal mechanism of homogeneous broadening is isolated, and deductions are made regarding inhomogeneous effects.

2. Experimental

Single-crystal boules of Nd^{3+}:$CaWO_4$ were grown by the Czochralski process [1] by I.R.D. of Newcastle upon Tyne, who used vacancy-incorporation to achieve charge neutrality. Specimens were grown having neodymium concentrations from 0.02 to 1%†, these concentrations being subsequently verified by spectrographic analysis. The trivalent neodymium ions substitute at divalent calcium sites [2, 3], the excess charges on each pair of neodymium ions being neutralized by the incorporation of one calcium vacancy.

Paramagnetic resonance of the neodymium ion in calcium tungstate occurs between the Zeeman levels of the lowest doublet of the ground manifold $^4I_{9/2}$ [4]. Higher levels of this multiplet occur at 114, 161, 230 and 471 cm^{-1} [5], all unpopulated at 4.2 K. The resonance was observed using a 35 GHz superheterodyne spectrometer [6, 7] with phase-sensitive detection at 160 kHz being used to record the first derivative of the resonance line. Specimens were cut to fit the Q-band waveguide, each specimen becoming its own resonant cavity with an unloaded Q of about 400 [8]. The *c*-axis of the specimen was made perpendicular to the narrow face of the waveguide and the static magnetic field lay in the *a-c* plane. All measurements of absorption lineshapes were made at liquid helium temperature because, at temperatures above about 10 K, spin-lattice relaxation leads to appreciable line-broadening. Relaxation time measurements were made at 4.2 K using the pulse saturation method [9]; recovery curves were photographed and plotted semi-logarithmically to extract the relaxation time.

*Present address: The Plessey Co Ltd, Allen Clark Research Centre, Caswell, Towcester, Northants.
†The concentration figures reported in this paper refer to the percentage of calcium sites occupied by neodymium.

3. Experimental results

In addition to the strong central absorption line, the eight lines of the hyperfine spectrum [10] were resolved. To a first-order approximation, these do not interfere with the central line and will be neglected in the subsequent linewidth analysis. Previous workers [11,12] have observed an additional orthorhombic spectrum in those specimens which have been charge-neutralized by vacancy incorporation. We have not observed such a spectrum and we can only conclude that its intensity is too low for our spectrometer to detect. The concentration dependence of ΔH_{ms} (the derivative peak-to-peak width) is shown in Fig. 1. From this figure it can be seen that the linewidth is a well-behaved function of the neodymium concentration.

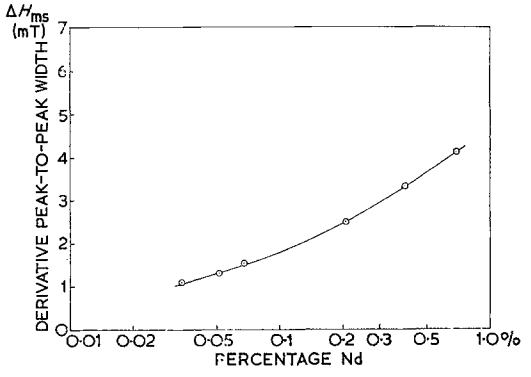

Figure 1 Experimentally-determined linewidth at 4.2 K as a function of Nd concentration.

The angular variation of ΔH_{ms} is shown in Fig. 2. Here, linewidths were measured at 10° intervals between $\theta = 0°$ and $\theta = 90°$, θ being the angle between the magnetic field direction and the crystallographic c-axis. Although the lineshapes for all the samples were good at values of θ around 0° and 90°, they were very poor between 25° and 45°. A similar observation for Nd^{3+}:$CaMoO_4$ has been reported by Kurkin and Shekun [13] over the whole range of polar angles. They have attributed this excess broadening and poor lineshape to the presence of neighbouring satellite lines which are ignored in their theoretical treatment. We have not observed any satellite lines in $CaWO_4$, but we will be discussing the excess broadening in a later section.

Spin-lattice relaxation times were measured as

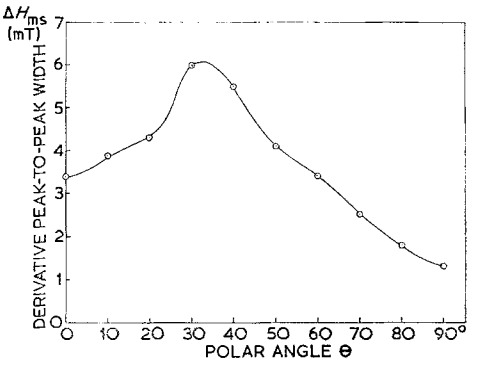

Figure 2 Experimentally-determined angular variation of linewidth at 4.2 K; 0.068% Nd.

a function of polar angle, and the results are plotted in Fig. 3. This behaviour was typical of all the samples measured. In every case there was a local minimum in T_1 around 30° superimposed upon a steady increase from 0 to 90°. With the exception of the local minimum, this behaviour has been observed before [14] and has been explained by deriving a mathematical angular dependence of the Direct (single-phonon) relaxation process known to be operative at 4.2 K in $CaWO_4$ [15]. Again, we shall return to the anomaly at $\theta = 30°$ in a later section.

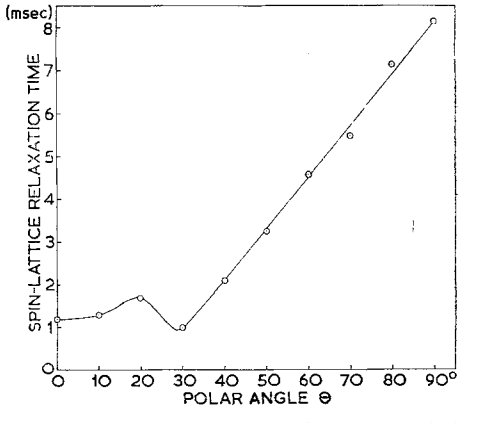

Figure 3 Experimentally-determined angular variation of spin-lattice relaxation time at 4.2 K; 0.068% Nd.

Having presented experimental results of linewidth and relaxation we shall now turn to a quantitative treatment of the possible underlying effects and attempt to correlate the theore-

tical values of the linewidth with those from the experimental work.

4. Theory

4.1. Introduction

Following the work of Grant and Strandberg [16] on Cr^{3+}:Al_2O_3, and that of Kurkin and Shekun [13] on Nd^{3+}:$CaMoO_4$ we shall assume that, of the homogeneous line-broadening mechanisms (i.e. those which act on every spin in the system), dipolar broadening will play a major part. With this as a starting point we can supply the second moment theory of Van Vleck [17] to the three dipolar interactions present in Nd^{3+}:$CaWO_4$ namely, Nd-W, Nd-Ca and Nd-Nd. We would expect the Nd-Nd interaction to be predominant at the higher concentrations but, to evaluate the total second moment, we must also investigate the other two interactions.

4.2. Second moments

Van Vleck's second moment theory concerns two different types of dipolar interaction: the interaction between atoms having the same g-factor and the same spin quantum number S; the interaction between atoms of different g and S, where the resonances of the two atoms do not overlap. If we assume that the magnetic moment in all cases is characterized by $g\sqrt{[S(S+1)]}$ where $g = 2$, we can write explicit equations for the second moments in the two cases. For like atoms;

$$\langle \Delta\omega^2 \rangle = \tfrac{3}{4} S(S+1)(g^2\beta^2/\hbar)^2 \Sigma_k [(r_{jk}^{-6})(3\cos^2\theta_{jk} - 1)^2] \quad (1)$$

where $\langle \Delta\omega^2 \rangle$ is the second moment of the line, ω being measured in radians per second; g is the Landé g-factor of all the atoms; β is the Bohr magneton; r_{jk} is the radius vector from the reference atom j to all the neighbouring atoms labelled over k; θ_{jk} is the angle between the radius vector and a crystallographic reference axis. For unlike atoms:

$$\langle \Delta\omega^2 \rangle = \tfrac{1}{3} S(S+1)(gg'\beta^2/\hbar)^2 \Sigma_k [(r_{jk}^{-6})(3\cos^2\theta_{jk} - 1)^2] \quad (2)$$

where g refers to the reference atom; g' refers to the surrounding atoms.

The numerical factor $\frac{3}{4}$ in the equation for like atoms, and $\frac{1}{3}$ in the equation for unlike atoms shows that like atoms produce a mean square broadening which is $\frac{9}{4}$ times greater than that produced by unlike atoms. The reason for this is that the resonances of like atoms do overlap and thus enhance the mutual coupling [17, 18].

Equations 1 and 2 can each be split into two parts, the first relating only to the atomic parameters, the second describing the particular crystal system being investigated. Van Vleck evaluated the $(3\cos^2\theta_{jk} - 1)^2$ term by using direction cosines but we shall use associated Legendre polynomials (spherical harmonics). In this way, we can write:

$$(3\cos^2\theta - 1)^2 = \tfrac{4}{5} + \frac{32\pi}{21}\sum_m Y_{2,m}^*(\theta_H,\phi_H)\,.\,Y_{2,m}(\theta_k,\phi_k) + \frac{32\pi}{35}\sum_m Y_{4,m}^*(\theta_H,\phi_H)\,.\,Y_{4,m}(\theta_k,\phi_k). \quad (3)$$

θ_H and ϕ_H refer the static magnetic field to the crystal axes, while θ_k and ϕ_k refer the radius vector to the same axes. For a crystal with tetragonal symmetry, the only possible values of m are 0 and ± 4 [18]. Combining these with the standard equation

$$Y_{l,-m} = (-1)^m Y_{l,m}^*, \quad (4)$$

and substituting in Equation 3 we have

$$(3\cos^2\theta - 1)^2 = \tfrac{4}{5} + \frac{32\pi}{21}[Y_{2,0}^*(\theta_H,\phi_H)\,.\,Y_{2,0}(\theta_k,\phi_k)] + \frac{32\pi}{35}[Y_{4,0}^*(\theta_H,\phi_H)\,.\,Y_{4,0}(\theta_k,\phi_k)] + \frac{64\pi}{35}[Y_{4,4}^*(\theta_H,\phi_H)\,.\,Y_{4,4}(\theta_k,\phi_k)].$$

Thus in order to evaluate the basic term $(r_{jk}^{-6})(3\cos^2\theta_{jk} - 1)^2$ we need to index all the active sites within a given radius of our reference site, and calculate r, θ, ϕ for each one before performing the summations required. Our final equations become:

(a) for like atoms

$$\langle \Delta\omega^2 \rangle = \tfrac{3}{4} S(S+1)(g^2\beta^2/\hbar)^2 [\tfrac{4}{5}\sum_k (r_{jk}^{-6}) + \frac{32\pi}{21} Y_{2,0}^*(\theta_H,\phi_H)\sum_k (r_{jk}^{-6})\,Y_{2,0}(\theta_k,\phi_k) + \frac{32\pi}{35} Y_{4,0}^*(\theta_H,\phi_H)\sum_k (r_{jk}^{-6})\,Y_{4,0}(\theta_k,\phi_k) + \frac{64\pi}{35} Y_{4,4}^*(\theta_H,\phi_H)\sum_k (r_{jk}^{-6})\,Y_{4,4}(\theta_k,\phi_k)]\,; \quad (5)$$

(b) for unlike atoms

$$\langle \Delta\omega^2 \rangle = \tfrac{1}{3} S(S+1)(gg'\beta^2/\hbar)^2 [\tfrac{4}{5}\sum_k (r_{jk}^{-6}) + \frac{32\pi}{21} Y_{2,0}^*(\theta_H, \phi_H) \sum_k (r_{jk}^{-6}) Y_{2,0}(\theta_k, \phi_k) + \frac{32\pi}{35} Y_{4,0}^*(\theta_H, \phi_H) \sum_k (r_{jk}^{-6}) Y_{4,0}(\theta_k, \phi_k) + \frac{64\pi}{35} Y_{4,4}^*(\theta_H, \phi_H) \sum_k (r_{jk}^{-6}) Y_{4,4}(\theta_k, \phi_k)] . \quad (6)$$

The standard forms of the spherical harmonics are well known [19] and are specified completely by θ and ϕ.

The mean square width of the line, as given by Equations 5 and 6 must be converted into the derivative peak-to-peak width (ΔH_{ms} of Figs. 1 and 2) for comparison with experimental results. ΔH_{ms} in hertz is given [16] by

$$\Delta H_{ms} = \sqrt{(\langle \Delta\omega^2 \rangle)}/\pi \text{ Hz.} \quad (7)$$

To convert this frequency width into a magnetic field width the parameter $\partial\nu/\partial H$ must be calculated from the experimental evaluation of g as a function of polar angle in Nd^{3+}:$CaWO_4$. Then

$$\Delta H_{ms} = \frac{\sqrt{(\langle \Delta\omega^2 \rangle)}}{\pi} \cdot \frac{\partial H}{\partial \nu} \text{ tesla.} \quad (8)$$

We shall concentrate first upon the crystal system and, having extracted r, θ, ϕ for substitution in the preceding equations, we shall then consider the specific values of S and g to be used for the particular dipolar interactions.

4.3. The crystal lattice

Calcium tungstate crystallizes in the tetragonal system [20] and has a space group $C_{4h}^6(I4_1/a)$ [21] with four molecules to the unit cell. The lattice parameters are $a = b = 5.243$ Å and $c = 11.376$ Å [22]. Each calcium atom is surrounded by eight oxygen atoms, but for the purposes of clarity, these have been omitted from the diagram of the unit cell, pictured in Fig. 4. The tungsten sites are indicated by circles and the calcium sites by crosses. The co-ordinate system is defined alongside the unit cell for ease of reference. We shall consider our neodymium reference atom at the origin of co-ordinates and use the eight unit cells having this atom as a common corner for our calculations. Taking more unit cells into the calculation does not significantly alter the results, as a later consideration of Tables I and II will show. In the Appendix there is a complete tabulation of the tungsten and calcium sites, together with their r, θ, ϕ values. Reference to this table is necessary to understand the simplifications that will occur by virtue of symmetry in the evaluation of the spherical harmonics.

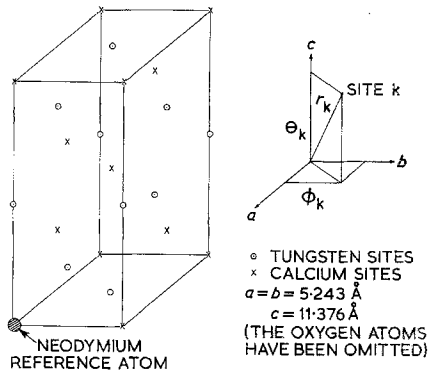

Figure 4 The calcium tungstate unit cell and the polar co-ordinate system.

4.4. The neodymium-neodymium interaction

In this case, because the dipolar interaction involves like atoms, Equation 5 must be used. The neodymium substitutes for calcium in the $CaWO_4$ lattice, these calcium sites lying on the surfaces of ten spheres. The appropriate r, θ, ϕ values are given in the Appendix. The values of θ for those sites on any given sphere are different, but take the form of θ or $(\pi - \theta)$. Because of the symmetry properties of the spherical harmonics, these angles produce the same values of $Y_{l,m}$. The situation regarding the equivalence of different ϕ angles on a given sphere is complicated by the presence of the factor $\exp(j4\phi)$ in $Y_{4,4}$. However, it is found that the sites occur in pairs, one having a $Y_{4,4}$ of the form $x + jy$ and the other having a $Y_{4,4}$ of the form $x - jy$. In this way, individual terms are complex but, under summation, the total value is always real. Table I shows the various radii of the spheres, the operative θ and ϕ values, the number of sites at each radius, the particular values of the spherical harmonics, and the summations required for substitution in Equation 5.

In Section 4.2 we noted that a basic premise for the validity of Equations 5 and 6 was that the magnetic moments of the surrounding atoms should be characterized by $g\sqrt{S}\ (S+1)$.

TABLE I Trigonometrical parameters for the calcium sites in 8 unit cells of $CaWO_4$, the origin or co-ordinates being the common corner of the unit cells.

r (Å)	θ_K (degrees)	ϕ_K (degrees)	N	$Y_{2,0}$ (θ_K, ϕ_K)	$Y_{4,0}$ (θ_K, ϕ_K)	$Y_{4,4}$ (θ_K, ϕ_K)	Nr^{-6} ($\times 10^{45}$ cm^{-6})	$Nr^{-6}Y_{2,0}$ ($\times 10^{45}$ cm^{-6})	$Nr^{-6}Y_{2,0}$ ($\times 10^{45}$ cm^{-6})	$Nr^{-6}Y_{4,4}$ ($\times 10^{45}$ cm^{-6})
3.868	42.67	90.00	4	0.1961	−0.3162	0.0830	1.1944	0.2342	−0.3777	0.1111
5.243	90.00	0 & 90	4	−0.3154	0.3174	0.4425	0.1926	−0.0607	0.0611	0.0852
6.515	64.12	26.57	8	−0.1351	−0.1529	−0.0813	0.1046	−0.0141	−0.0160	−0.0085
6.790	33.10	45.00	8	0.3486	−0.0863	−0.0394	0.0816	0.0285	−0.0070	−0.0032
7.415	90.00	45.00	4	−0.3154	0.3174	−0.4425	0.0241	−0.0076	0.0076	−0.0107
8.926	17.08	0.00	4	0.5492	0.5088	0.0033	0.0079	0.0043	0.0040	0.0000
10.352	34.49	63.43	8	−0.3274	−0.1298	−0.0128	0.0065	0.0021	−0.0008	−0.0001
11.376	0.00	—	2	0.6308	0.8463	0.0000	0.0009	0.0006	0.0008	0.0000
12.526	24.74	0 & 90	8	0.4651	0.2188	0.0136	0.0021	0.0010	0.0005	0.0000
13.579	33.10	45.00	8	0.3486	−0.0863	−0.0394	0.0013	0.0005	−0.0001	−0.0001
						Sum	1.6160	0.1887	−0.3276	0.1738

TABLE II Trigonometrical parameters for the tungsten sites in 8 unit cells of $CaWO_4$, the origin of co-ordinates being the common corner of the unit cells.

r (Å)	θ_K (degrees)	ϕ_K (degrees)	N	$Y_{2,0}$ (θ_K, ϕ_K)	$Y_{4,0}$ (θ_K, ϕ_K)	$Y_{4,4}$ (θ_K, ϕ_K)	Nr^{-6} ($\times 10^{45}$ cm^{-6})	$Nr^{-6}Y_{2,0}$ ($\times 10^{45}$ cm^{-6})	$Nr^{-6}Y_{44,0}$ ($\times 10^{45}$ cm^{-6})	$Nr^{-6}Y_{4,4}$ ($\times 10^{45}$ cm^{-6})
3.707	90.00	45.00	4	−0.3154	0.3174	−0.4425	1.5414	−0.4826	0.4892	−0.6821
3.868	42.67	0.00	4	0.1961	−0.3162	0.0930	1.1944	0.2342	−0.3777	0.1111
5.688	0.00	—	2	0.6308	0.8463	0.0000	0.0591	0.0373	0.0500	0.0000
6.515	64.12	63.43	8	−0.1351	−0.1529	−0.0813	0.1046	−0.0141	−0.0160	−0.0085
7.736	42.67	90 & 0	8	0.1961	−0.3162	0.0930	0.0373	0.0073	−0.0118	0.0035
8.926	17.08	90.00	4	0.5492	0.5088	0.0033	0.0079	0.0043	0.0040	0.0000
9.345	52.51	45.00	8	0.0351	−0.3502	−0.1754	0.0120	0.0042	−0.0042	−0.0021
10.352	34.49	26.57	8	0.3274	−0.1298	−0.0128	0.0065	0.0021	−0.0008	−0.0001
11.965	18.05	45.00	8	0.5399	0.4742	−0.0041	0.0027	0.0015	0.0013	−0.0000
						Sum	2.9659	−0.2131	0.1341	−0.5782

However, for neodymium, the ground manifold is $^4I_{9/2}$ giving $J = 9/2$ and $L = 6$. Because of the spin-orbit coupling, the magnetic moment becomes $g\sqrt{[J(J+1)]}$ with $g = 8/11$ [23]. Thus, Equation 5 is modified to become:

$$\begin{aligned}\langle \Delta\omega^2 \rangle = {} & \tfrac{3}{4} J(J+1)(g^2\beta^2/\hbar)^2 \\ & \times 10^{45}\,[1.2928 + 0.9032\, Y_{2,0}{}^*(\theta_H, \phi_H) \\ & - 0.9411\, Y_{4,0}{}^*(\theta_H, \phi_H) \\ & + 0.9866\, Y_{4,4}{}^*(\theta_H, \phi_H)]. \end{aligned} \quad (9)$$

From Equation 4 it can be seen that $Y_{2,0}{}^* = Y_{2,0}$ and $Y_{4,0}{}^* = Y_{4,0}$ and we can make $Y_{4,4}{}^* = Y_{4,4}$ by taking $\phi = 0°$. In this way Equation 9 becomes totally real. Substituting values in the first part of Equation 9 gives:

$$\begin{aligned}& \tfrac{3}{4} J(J+1)(g^2\beta^2/\hbar)^2 \\ & \quad = 3.453 \times 10^{-26}\,(\text{rad sec}^{-1})^2\,\text{cm}^6. \end{aligned} \quad (10)$$

In order to make this calculation directly comparable with the experimental data, n (the concentration of active sites) must be chosen accordingly. The Van Vleck formulae assume that all the surrounding sites involved in the summation are occupied. In other words, they assume the concentration to be 100%. To allow for lower concentrations, the factor n is introduced directly into Equation 9.

We now have two separate cases to consider: firstly, the variation of linewidth with neodymium concentration at $\theta = 90°$; secondly, the variation of the linewidth with polar angle at constant concentration. The first condition requires that n is changed over the range of values of the specimens, namely 0.02 to 1% neodymium ($n = 0.0002$ to $n = 0.01$). The second condition requires that n is held constant at 0.000 68, the concentration of the specimen used in the polar angle plot of Fig. 2. Using these values of n and θ together with the spherical harmonics from Table I, the graphs of Figs. 5 and 6 are produced. The full lines relate to the theoretical results and the broken lines show the experimental curves.

4.5. The neodymium-tungsten and neodymium-calcium interactions

Similar calculations were made for the Nd-W and the Nd-Ca interactions. For Nd-W, Equation 6 is applicable, and using the figures from Table II we have:

$$\langle \Delta\omega^2 \rangle = \tfrac{1}{3} S(S+1)(gg'\beta^2/\hbar)^2 \times 10^{45} [2.374 - 1.020\, Y_{2,0}(\theta_H, \phi_H) + 0.385\, Y_{4,0}^*(\theta_H, \phi_H) - 3.322\, Y_{4,4}^*(\theta_H, \phi_H)]. \quad (11)$$

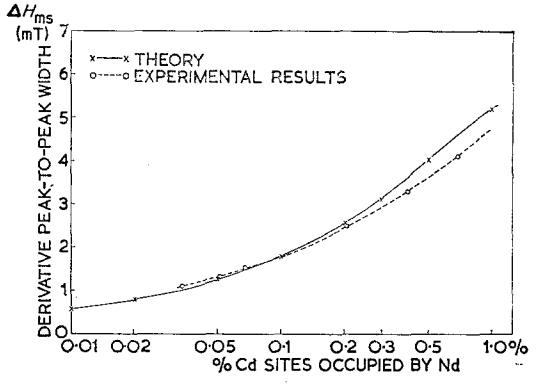

Figure 5 Concentration dependence of the Nd-Nd dipolar broadening at $\theta = 90°$ and 4.2 K.

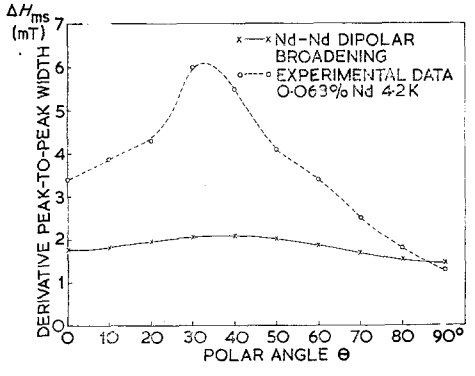

Figure 6 Angular variation of linewidth.

For the tungsten nucleus, the g-value can be derived from NMR tables to be 0.23 but, for inclusion in Equation 11 it must be multiplied by the ratio of the nuclear magneton to the Bohr magneton, i.e. 1/1836. Thus $g' = 1.252 \times 10^{-4}$. For naturally-occurring tungsten, the abundance of the ^{183}W isotope of nuclear spin $s = \frac{1}{2}$ is 14%, so we must include the factor $n = 0.14$ directly into Equation 11:

$$\tfrac{1}{3} S(S+1)(gg'\beta^2/\hbar)^2 n = 1.930 \times 10^{-36} (\text{rad sec}^{-1})^2 \text{ cm}^6. \quad (12)$$

The dipolar broadening given by this calculation varies from about 7×10^{-7} T at $\theta = 0°$ to about 5×10^{-7} T at $\theta = 90°$, values which can be neglected in comparison with those of the previous section.

Using the indexed calcium sites in the Appendix together with Table I we arrive at dipolar broadenings for the Nd-Ca interaction which are of the same order as those of the Nd-W interaction, some 5000 times smaller than the Nd-Nd interaction.

5. Discussion

By considering the homogeneous broadening due to dipolar interactions in neodymium-doped calcium tungstate we have produced the concentration dependence and the angular dependence shown in Figs. 5 and 6. As these figures show, the concentration dependence is in very good agreement with experiment, but the angular dependence coincides with experiment only at $\theta = 90°$. This, however, is to be expected because 90° is the optimum orientation for the reduction of inhomogeneous broadening mechanisms [8]. Bearing this in mind, it can be said that the linewidth and its concentration dependence are fully explained at $\theta = 90°$ by dipolar broadening. The total dipolar broadening is given by the square root of the sum of the second moments of the three individual dipolar interactions. The Nd-Nd interaction is predominant by a factor of about 5000. This agreement between theory and experiment would suggest that the other major causes of homogeneous broadening, spin-lattice relaxation and exchange interaction, are negligible in this case. For relaxation broadening, take Fig. 3: the minimum value of relaxation time is about 1 msec, corresponding to a broadening of 159 Hz. Comparing this with the Nd-Ca dipolar width (the smallest of the three contributions) of between 5.2 and 6.9 kHz shows that relaxation broadening can be neglected. Exchange interactions also can be ignored because of the screened position of the $4f$ electrons in neodymium.

As the polar angle θ is changed from 90°, inhomogeneous mechanisms should become increasingly important. Kurkin and Shekun [13] have shown that, in Czochralski-grown Nd^{3+}:$CaMoO_4$, the major inhomogeneous broadening mechanism is axial misorientation, manifesting itself as a spread in θ through the specimen. Values of this misorientation were quoted as 1.5° for a 0.05% Nd concentration and 4° for a 0.5% Nd concentration. From our own investigation on Nd^{3+}:$CaWO_4$, we estimate the axial misorientation in the 0.068% Nd sample to be 57 minutes of arc. Using this as $\Delta\theta$ in the equation

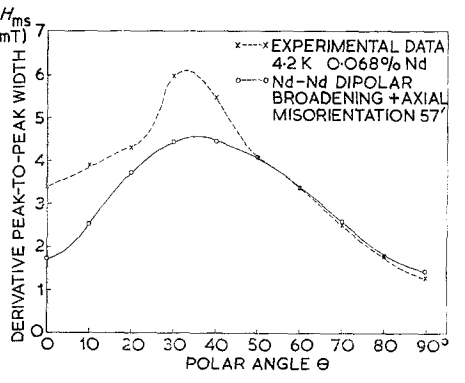

Figure 7 Angular variation of linewidth.

$$(\Delta H_{\mathrm{ms}})^2_{\mathrm{total}} = [\Delta H(\theta)]^2 + \left[\Delta\theta \cdot \frac{\mathrm{d}H}{\mathrm{d}\theta}\right]^2, \quad (13)$$

where $\Delta H(\theta)$ is the homogeneous width from Fig. 6 and $\mathrm{d}H/\mathrm{d}\theta$ is determined from experiment, the graph of Fig. 7 is obtained. This shows very good agreement between 50 and 90°, but the fit is less good between 25 and 40°. It is interesting to note that there is a pronounced peak in the experimental linewidth around 30°, the polar angle at which there is a pronounced dip in the relaxation time (Fig. 3). This is possible evidence for the existence of cross-relaxation: Larson and Jeffries [24] have reported such a dip in the angular variation of relaxation time in a neodymium-doped rare-earth double salt, and have ascribed it to cross-relaxation to cerium, a common impurity in neodymium. It is likely that we are observing the same thing here. Although there is no direct evidence at the present time, it is reasonable to suppose that the remaining discrepancy between $\theta = 0$ and 20° will be owing to the residual effects of inhomogeneous broadening owing to internal crystal strain and electric field effects.

6. Conclusions

Experimental results are given relating to the linewidths of the neodymium resonance at 35 GHz in Nd^{3+}: $CaWO_4$ as a function of polar angle and neodymium concentration. By comparing these with the results of dipolar broadening theory, it is shown that the Nd-Nd interaction is the predominant homogeneous broadening mechanism, accounting for the total linewidth at a polar angle of 90° where inhomogeneous mechanisms are minimized. The concentration dependence also is explained by the Nd-Nd interaction. The angular dependence of the linewidth is shown to be dominated by one inhomogeneous mechanism, the axial misorientation of the $CaWO_4$ crystal. The remaining linewidth anomaly is correlated with a similar anomaly in the angular dependence of the spin-lattice relaxation time, suggesting that cross-relaxation is also present.

Appendix

Taking 8 unit cells of $CaWO_4$ with their common corner taken as the origin of the polar co-ordinate system (see Fig. 4), the tungsten and the calcium sites can be indexed.

(a) The tungsten sites

a	b	c	r (Å)	θ°	ϕ°
$\frac{1}{2}$	$\frac{1}{2}$	0	3.707	90.00	45.00
$-\frac{1}{2}$	$\frac{1}{2}$	0	3.707	90.00	135.00
$-\frac{1}{2}$	$-\frac{1}{2}$	0	3.707	90.00	225.00
$\frac{1}{2}$	$-\frac{1}{2}$	0	3.707	90.00	315.00
$\frac{1}{2}$	0	$\frac{1}{4}$	3.868	42.67	0.00
$-\frac{1}{2}$	0	$\frac{1}{4}$	3.868	42.67	180.00
0	$\frac{1}{2}$	$-\frac{1}{4}$	3.868	137.33	90.00
0	$-\frac{1}{2}$	$-\frac{1}{4}$	3.868	137.33	270.00
0	0	$\frac{1}{2}$	5.688	0.00	—
0	0	$-\frac{1}{2}$	5.688	180.00	—
$\frac{1}{2}$	1	$\frac{1}{4}$	6.515	64.12	63.43
$-\frac{1}{2}$	1	$\frac{1}{4}$	6.515	64.12	116.57
$-\frac{1}{2}$	-1	$\frac{1}{4}$	6.515	64.12	243.43
$\frac{1}{2}$	-1	$\frac{1}{4}$	6.515	64.12	296.57
0	$\frac{1}{2}$	$\frac{3}{4}$	8.926	17.08	90.00
0	$-\frac{1}{2}$	$\frac{3}{4}$	8.926	17.08	270.00
$\frac{1}{2}$	0	$-\frac{3}{4}$	8.926	162.92	0.00
$-\frac{1}{2}$	0	$-\frac{3}{4}$	8.926	162.92	180.00
1	1	$\frac{1}{2}$	9.345	52.51	45.00
-1	1	$\frac{1}{2}$	9.345	52.51	135.00
-1	-1	$\frac{1}{2}$	9.345	52.51	225.00
1	-1	$\frac{1}{2}$	9.345	52.51	315.00
1	1	$-\frac{1}{2}$	9.345	127.49	45.00
-1	1	$-\frac{1}{2}$	9.345	127.49	135.00
-1	-1	$-\frac{1}{2}$	9.345	127.49	225.00
1	-1	$-\frac{1}{2}$	9.345	127.49	315.00
1	$\frac{1}{2}$	$\frac{3}{4}$	10.352	34.49	26.57
-1	$\frac{1}{2}$	$\frac{3}{4}$	10.352	34.49	153.43
-1	$-\frac{1}{2}$	$\frac{3}{4}$	10.352	34.49	206.57

contd.

a	b	c	r(Å)	$\theta°$	$\phi°$
1	$\frac{1}{2}$	$-\frac{1}{4}$	6.515	115.88	26.57
-1	$\frac{1}{2}$	$-\frac{1}{4}$	6.515	115.88	153.43
-1	$-\frac{1}{2}$	$-\frac{1}{4}$	6.515	115.88	206.57
1	$-\frac{1}{2}$	$-\frac{1}{4}$	6.515	115.88	333.43
0	1	$\frac{1}{2}$	7.736	42.67	90.00
1	0	$\frac{1}{2}$	7.736	42.67	0.00
-1	0	$\frac{1}{2}$	7.736	42.67	180.00
0	-1	$\frac{1}{2}$	7.736	42.67	270.00
0	1	$-\frac{1}{2}$	7.736	137.33	90.00
1	0	$-\frac{1}{2}$	7.736	137.33	0.00
-1	0	$-\frac{1}{2}$	7.736	137.33	180.00
0	-1	$-\frac{1}{2}$	7.736	137.33	270.00

a	b	c	r(Å)	$\theta°$	$\phi°$
1	$-\frac{1}{2}$	$\frac{3}{4}$	10.352	34.49	333.43
$\frac{1}{2}$	1	$-\frac{3}{4}$	10.352	145.51	63.43
$-\frac{1}{2}$	1	$-\frac{3}{4}$	10.352	145.51	116.57
$-\frac{1}{2}$	-1	$-\frac{3}{4}$	10.352	145.51	243.43
$\frac{1}{2}$	-1	$-\frac{3}{4}$	10.352	145.51	296.57
$\frac{1}{2}$	$\frac{1}{2}$	—	11.965	18.05	45.00
$-\frac{1}{2}$	$\frac{1}{2}$	1	11.965	18.05	135.00
$-\frac{1}{2}$	$-\frac{1}{2}$	1	11.965	18.05	225.00
$\frac{1}{2}$	$-\frac{1}{2}$	1	11.965	18.05	315.00
$\frac{1}{2}$	$\frac{1}{2}$	-1	11.965	161.95	45.00
$-\frac{1}{2}$	$\frac{1}{2}$	-1	11.965	161.95	135.00
$-\frac{1}{2}$	$-\frac{1}{2}$	-1	11.965	161.95	225.00
$\frac{1}{2}$	$-\frac{1}{2}$	-1	11.965	161.95	315.00

(b) The calcium sites

a	b	c	r(Å)	$\theta°$	$\phi°$
0	$\frac{1}{2}$	$\frac{1}{4}$	3.868	42.67	90.00
0	$-\frac{1}{2}$	$\frac{1}{4}$	3.868	42.67	270.00
$\frac{1}{2}$	0	$-\frac{1}{4}$	3.868	137.33	0.00
$-\frac{1}{2}$	0	$-\frac{1}{4}$	3.868	137.33	180.00
0	1	0	5.243	90.00	90.00
1	0	0	5.243	90.00	0.00
-1	0	0	5.243	90.00	180.00
0	-1	0	5.243	90.00	225.00
1	$\frac{1}{2}$	$\frac{1}{4}$	6.515	64.12	26.57
-1	$\frac{1}{2}$	$\frac{1}{4}$	6.515	64.12	153.43
-1	$-\frac{1}{2}$	$\frac{1}{4}$	6.515	64.12	206.57
1	$-\frac{1}{2}$	$\frac{1}{4}$	6.515	64.12	333.43
$\frac{1}{2}$	1	$-\frac{1}{4}$	6.515	115.88	63.43
$-\frac{1}{2}$	1	$-\frac{1}{4}$	6.515	115.88	116.57
$-\frac{1}{2}$	-1	$-\frac{1}{4}$	6.515	115.88	243.43
$\frac{1}{2}$	-1	$-\frac{1}{4}$	6.515	115.88	296.57
$\frac{1}{2}$	$\frac{1}{2}$	$\frac{1}{2}$	6.790	33.10	45.00
$-\frac{1}{2}$	$\frac{1}{2}$	$\frac{1}{2}$	6.790	33.10	135.00
$-\frac{1}{2}$	$-\frac{1}{2}$	$\frac{1}{2}$	6.790	33.10	225.00
$\frac{1}{2}$	$-\frac{1}{2}$	$\frac{1}{2}$	6.790	33.10	315.00
$\frac{1}{2}$	$\frac{1}{2}$	$-\frac{1}{2}$	6.790	146.90	45.00
$-\frac{1}{2}$	$\frac{1}{2}$	$-\frac{1}{2}$	6.790	146.90	135.00
$-\frac{1}{2}$	$-\frac{1}{2}$	$-\frac{1}{2}$	6.790	146.90	225.00
$\frac{1}{2}$	$-\frac{1}{2}$	$-\frac{1}{2}$	6.790	146.90	315.00
1	1	0	7.415	90.00	45.00
-1	1	0	7.415	90.00	135.00
-1	-1	0	7.415	90.00	225.00
1	-1	0	7.415	90.00	315.00

a	b	c	r(Å)	$\theta°$	$\phi°$
$\frac{1}{2}$	0	$\frac{3}{4}$	8.926	17.08	0.00
$-\frac{1}{2}$	0	8	8.926	17.08	180.00
0	$\frac{1}{2}$	$-\frac{3}{4}$	8.926	162.92	90.00
0	$-\frac{1}{2}$	$-\frac{3}{4}$	8.926	162.92	270.00
$\frac{1}{2}$	1	$\frac{3}{4}$	10.352	34.49	63.43
$-\frac{1}{2}$	1	$\frac{3}{4}$	10.352	34.49	116.57
$-\frac{1}{2}$	-1	$\frac{3}{4}$	10.352	34.49	243.43
$\frac{1}{2}$	-1	$\frac{3}{4}$	10.352	34.49	296.57
1	$\frac{1}{2}$	$-\frac{3}{4}$	10.352	145.51	26.57
-1	$\frac{1}{2}$	$-\frac{3}{4}$	10.352	145.51	153.43
-1	$-\frac{1}{2}$	$-\frac{3}{4}$	10.352	145.51	206.57
1	$-\frac{1}{2}$	$-\frac{3}{4}$	10.352	145.51	333.43
0	0	1	11.376	0.00	—
0	0	-1	11.376	180.00	—
0	1	1	12.526	24.74	90.00
1	0	1	12.526	24.74	0.00
-1	0	1	12.526	24.74	180.00
0	-1	1	12.526	24.74	270.00
0	1	-1	12.526	155.26	90.00
1	0	-1	12.526	155.26	0.00
-1	0	-1	12.626	155.26	180.00
0	-1	-1	12.526	155.26	270.00
1	1	1	13.579	33.10	45.00
-1	1	1	13.579	33.10	135.00
-1	-1	1	13.579	33.10	225.00
1	-1	1	13.579	33.10	315.00
1	1	-1	13.579	146.90	45.00
-1	1	-1	13.579	146.90	135.00
-1	-1	-1	13.579	146.90	225.00
1	-1	-1	13.579	146.90	315.00

References

1. J. CZOCHRALSKI, *Z. Phys. Chem.* **92** (1918) 219.
2. U. RANON and V. VOLTERRA, *Phys. Rev.* **134** (1964) A1483.
3. J. KIRTON and P. A. FORRESTER, *J. Molecular. Spectrosc. (USA)* **22** (1967) 367.
4. E. CARLSON and G. H. DIEKE, *J. Chem. Phys.* **29** (1958) 229.

5. L. F. JOHNSON and R. A. THOMAS, *Phys. Rev.* **131** (1963) 2038.
6. G. BROWN, D. R. MASON and J. S. THORP, *J. Sci. Instrum.* **42** (1965) 648.
7. G. BROWN, Ph.D. Thesis University of Durham (1967).
8. C. J. KIRKBY, Ph.D. Thesis University of Durham (1967).
9. C. F. DAVIS, M. W. P. STRANDBERG and R. L. KYHL, *Phys. Rev.* **111** (1958) 1268.
10. U. RANON, *Phys. Letters* **8** (1964) 154.
11. M. P. KLEIN and W. B. MIMS, *Bull. Amer. Phys. Soc.* **7** (1962) 625.
12. C. G. B. GARRETT and F. R. MERRITT, *Apl. Phys. Letters* **4** (1964) 31.
13. I. N. KURKIN and L. YA. SHEKUN, *Sov. Phys. Sol. Stat.* **9** (1967) 339.
14. G. H. LARSON and C. D. JEFFRIES, *Phys. Rev.* **141** (1966) 461.
15. N. E. KASK, L. S. KORNIENKO, A. M. PROKHOROV and M. FAKIR, *Sov. Phys. Sol. Stat.* **5** (1964)1675.
16. W. J. C. GRANT and M. W. P. STRANDBERG, *Phys. Rev.* **135** (1964) A727.
17. J. H. VAN VLECK, *Phys. Rev.* **74** (1948) 1168.
18. B. BLEANEY and K. W. H. STEVENS, *Reports Progr. Phys* **16** (1953) 108.
19. D. C. MATTIS, "The Theory of Magnetism" (Harper and Row, New York, 1965).
20. R. W. G. WYCKOFF, "Crystal Structures" (Interscience, New York, 1948).
21. C. F. HEMPSTEAD and K. D. BOWERS, *Phys. Rev.* **118** (1960) 131.
22. A. ZALKIN and D. H. TEMPLETON, *J. Chem. Phys.* **40** (1964) 501.
23. N. CUSACK, "The Electrical and Magnetic Properties of Solids" (Longmans, London, 1960).
24. G. H. LARSON and C. D. JEFFRIES, *Phys. Rev.* **145** (1966) 311.

Received 12 June and accepted 16 July 1973